

All-fiber variable optical delay line for applications in optical coherence tomography: feasibility study for a novel delay line

EunSeo Choi, Jihoon Na, Seon Young Ryu, Gopinath Mudhana, and Byeong Ha Lee

*Department of Information and Communications
Gwangju Institute of Science and Technology
1, Oryong-dong, Buk-Gu, Gwangju, 500-712, Korea
leebh@gist.ac.kr*

Abstract: We have implemented an all-fiber optical delay line using two linearly chirped fiber Bragg gratings cascaded in reverse order and all-fiber optics components. The features of the proposed all-fiber based technique for variable delay line are discussed theoretically and demonstrated experimentally. The non-invasive cross-sectional images of biomedical samples as well as a transparent glass plate obtained with implemented all-fiber delay line having the axial resolution of 100 μm and the dynamic range of 50dB are presented to validate the imaging performance and demonstrate the feasibility of the delay line for optical coherence tomography.

©2005 Optical Society of America

OCIS codes: (170.4500) Optical coherence tomography; (110.4500) Optical coherence tomography; (120.3890) Medical optics instrumentation; (120.2340) Fiber optics components

References and links

1. D. Huang, E. A. Swanson, C. P. Lin, J. S. Schuman, W. G. Stinson, W. Chang, M. R. Hee, T. Flotte, K. Gregory, C. A. Puliafito, and J. G. Fujimoto, "Optical coherence tomography," *Science* **254**, 1178-1181 (1991).
2. A. M. Rollins, S. Yazdanfar, M. D. Kulkarni, R. U.-Arunyawee, and J. A. Izatt, "In vivo video rate optical coherence tomography," *Opt. Express* **3**, 219-229 (1998).
<http://www.opticsexpress.org/abstract.cfm?URI=OPEX-3-6-219>
3. C. Froehly, B. Colombeau, and M. Vampouille, in *Progress In Optics* v. 20, ed. E. Wolf (North Holland, Amsterdam, 1983), pp. 63-153.
4. E. A. Swanson, D. Huang, M. R. Hee, J. G. Fujimoto, C. P. Lin, and C. A. Puliafito, "High speed optical coherence domain reflectometry," *Opt. Lett.* **17**, 151-153 (1992).
5. J. Ballif, R. Gianotti, Ph. Chavanne, R. Walti, and R. P. Salathe, "Rapid and scalable scans at 21m/s in optical low-coherence reflectometry," *Opt. Lett.* **22**, 757-759 (1997).
6. C. B. Su, "Achieving variation of the optical path length by a few millimeters at millisecond rates for imaging of turbid media and optical interferometry: a new technique," *Opt. Lett.* **22**, 665-667 (1997).
7. A. M. Rollins, R. U.-Arunyawee, A. Chak, C. K. Wong, K. Kobayashi, M. V. Sivak, Jr., J. A. Izatt, "Real-time in vivo imaging of human gastrointestinal ultrastructure by use of endoscopic optical coherence tomography with a novel efficient interferometer design," *Opt. Lett.* **24**, 1358-1360 (1999).
8. K. K. M. B. D. Silva, A. V. Zvyagin, and D. D. Sampson, "Extended range, rapid scanning optical delay line for biomedical interferometric imaging," *Electron. Lett.* **35**, 1404-1406 (1999).
9. G. J. Tearney, B. E. Bouma, S. A. Boppart, B. Golubovic, E. A. Swanson, and J. G. Fujimoto, "Rapid acquisition of in vivo biological Images using optical coherence tomography," *Opt. Lett.* **21**, 1408-1410 (1996).
10. V. M. Gelikonov, A. M. Sergeev, G. V. Gelikonov, F. I. Feldchtein, N. D. Gladkova, J. Ioannovich, K. Fragia, and T. Pirza, "Compact Fast-Scanning OCT Device for In Vivo Biotissue Imaging," in Conference on Lasers and Electro-Optics, Vol. 9 of 1996 OSA Technical Digest Series (Optical Society of America, Washington, D.C., 1996), pp.58-59.
11. B. H. Lee, T.-J. Eom, E. Choi, Y.-J. Kim, C. Lee, "All fiber delay line for OCT based on fiber gratings," in Asian Symposium on Biomedical Optics and Photomedicine (BOPM 2002), TB2-1(Optical Society of America, SPIE, Sapporo, 2002), pp.140-141.
12. B. H. Lee, T.-J. Eom, E. Choi, G. Mudhana, C. Lee, "Novel Optical Delay Line for Optical Coherence Tomography System," *Opt. Rev.* **10**, 572-575 (2003).

13. C. Yang, S. Yazdanfar, and J. Izatt, "Amplification of optical delay by use of matched linearly chirped fiber Bragg gratings," *Opt. Lett.* **29**, 685-687 (2004).
14. F. Ouellette, "Dispersion cancellation using linearly chirped Bragg grating in optical waveguides," *Opt. Lett.* **12**, 847-849 (1987).
15. R. Kashyap, *Fiber Bragg gratings* (Academic Press, New York, 1999), pp.311-354.
16. Y. Pan, J. Welzel, R. Bringruber, and R. Engelhardt, "Optical coherence-gated imaging of biomedical tissues," *IEEE J. Sel. Top. Quant. Elect.* **2**, 1029-1034 (1996).
17. P.-L. Hsiung, X. Li, C. Chudoba, I. Hartl, T. H. Ko, and J. G. Fujimoto, "High-speed path-length scanning with a multiple-pass cavity delay line," *App. Opt.* **2**, 640-648 (2003).
18. W. W. Morey, J. R. Dunphy, and G. Meltz, "Multiplexing fiber Bragg gratings sensors," in *Distributed and Multiplexed Fiber optic Sensors*, Donald C. O'Shea, ed., *Proc. SPIE* **1586**, 216-224 (1991).
19. T. Imai, T. Komukai, and M. Nakazawa, "Dispersion tuning of a linearly chirped fiber Bragg grating without a center wavelength shift by applying a strain gradient," *IEEE Photon. Technol. Lett.* **10**, 845-847 (1998).
20. J. Kim, J. Bae, Y.-G. Han, S. H. Kim, J.-M. Jeong, and S. B. Lee, "Effectively Tunable Dispersion Compensation Based on Chirped Fiber Bragg Gratings Without Central Wavelength Shift," *IEEE Photon. Technol. Lett.* **16**, 849-851 (2004).
21. M. Sumetsky, P. S. Westbrook, P. I. Reyes, N. M. Litchinitser, B. J. Eggleton, Y. Li, R. Deshmukh, C. Socolich, F. Rosca, J. Bennike, F. Liu, and S. Dey, "Reduction of chirped fiber grating group delay ripple penalty through UV post processing," *Optical Fiber Communication Conference Postdeadline Papers PD28-1*, OSA, Washington DC (2003).
22. P. I. Reyes, M. Sumetsky, N. M. Litchinitser, and P. S. Westbrook, "Reduction of group delay ripple of multi-channel chirped fiber gratings using adiabatic UV correction," *Opt. Express* **12**, 2676- 2687 (2004).
<http://www.opticsexpress.org/abstract.cfm?URI=OPEX-12-12-2676>

1. Introduction

Optical coherence tomography (OCT) is one of the image modalities for biomedical imaging. It enables obtaining non-invasive cross-sectional images of turbid samples as well as transparent media with a resolution of up to few micrometers [1]. As an image modality capable of high-speed scanning, OCT can support *in vivo* real-time imaging of biomedical specimens at video rate [2]. Therefore, developing a high-speed optical delay line (ODL) is determinant in achieving the real-time imaging. ODL that plays an important role in various other fields such as characterization of ultra-fast laser pulses [3] and path length-resolved measurement of reflectivity [4] has adapted various schemes to provide a long enough optical delay at a high repetition rate.

The simplest scheme of ODL uses a mirror mounted on a linear oscillator. This technique provides a long optical delay by using a stage with long traveling length but low scanning speed is a serious problem. Although angular scanning method using a rotating glass cube has achieved a very high scan speed at a high repetition rate (21 m/s at 384 Hz), the drawbacks such as non-linearity in the optical delay and delay-dependent dispersion have limited its use [5, 6]. As a popular ODL scheme for OCT, Fourier domain optical delay line or rapid scanning optical delay line (RSODL), which was originally used for pulse stretching or compression, has been developed to obtain a high-speed axial scanning suitable for real-time imaging [7, 8]. RSODL that is composed of a diffraction grating, focusing lens, and a scanning mirror provides a large optical delay and high speed axial scanning with a linear phase ramp in the frequency domain. Despite the successful implementations of these techniques in OCT, they are bulk-optic components based configurations; they have the inherent problems of system complexity, alignment difficulty, and dispersion mismatch. A fiber-based ODL can overcome these problems and have advantages of compactness and low power loss. A technique utilizing optical fiber coiled around a piezoelectric transducer (PZT) drum has been reported [9, 10]. By operating the PZT at a rate of 500 Hz, real-time imaging (4 frames/sec) [9] with about 3-mm delay was achieved. However, stretching the coiled fiber induces severe birefringence and also possess temperature drift problem.

In this paper, we present the characteristics of an all-fiber optical delay line (AFODL) based on chirped fiber gratings and demonstrate the feasibility of the AFODL for OCT application with the OCT images acquired using the delay line. The proposed variable ODL implemented is all-fiber and offers amplified optical delay without the drawbacks of the

coiled fiber based ODL, and possess all the inherent merits of a fiber-based delay line such as alignment-free, lower optical power loss, and compactness. We explain the characteristics of the proposed AFODL using the fundamental distributive reflection nature of a CFBG, and confirm the theoretical principles by comparing with the experimental results. We have acquired the cross sectional images of a transparent cover glass and biological samples using the AFODL based OCT system. The OCT images thus acquired validate the potential and feasibility of the proposed delay line as an alternative technique for an OCT delay line. It can be noted that the proposed scheme and its main concept are based on the theoretical analysis given by B.H. Lee *et al.* [11, 12] and independently performed by C. Yang *et al.* [13].

2. The principle of all-fiber optical delay line

2.1 Introduction to chirped fiber Bragg gratings

Chirped fiber Bragg grating (CFBG) has been widely used as a chromatic dispersion compensator in optical communication systems since the possibility was first reported in 1987 [14]. While a fiber Bragg grating (FBG) has the same grating period Λ along its whole length, the grating period of a CFBG varies along its length. The period in a CFBG can take any functional form such as linear, quadratic or even higher order. Among them, linearly chirped FBGs are popular due to its linear group delay property that can be used for performing dispersion compensation. Owing to the varying period, the spectrum of the CFBG is much broad compared than that of a FBG.

In a CFBG, different wavelength components of an incident light are reflected at different positions along the grating according to the local grating period [15]

$$\lambda_B(z) = 2 n_{\text{eff}} \Lambda(z). \quad (1)$$

Where, $\lambda_B(z)$ is the reflection wavelength, or a Bragg wavelength, at a position z along the gratings, n_{eff} is the effective refractive index of the core mode, and $\Lambda(z)$ is the local grating period. The position dependent or distributive reflection characteristic of the CFBG is depicted in Fig. 1(a). The figure states that the shorter wavelength component λ_s is reflected earlier than the longer one λ_L . The associated reflection spectrum and dispersion curve of the CFBG used for this experiment are shown in Fig. 1(b). The distributive reflection property of the CFBG not only provides a broad reflection spectrum but also gives a linear group delay that can be exploited to obtain variable time delay that will be shown in the following section.

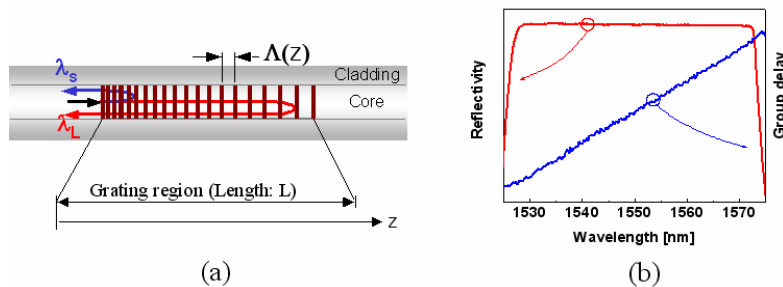


Fig. 1. (a) The schematic of a linearly chirped FBG and (b) the measured reflectivity and the group delay of the CFBGs used in the experiment.

2.2 The theory of CFBG based delay line

The CFBG-based delay line has been proposed and developed to realize AFODL for optical coherence tomography applications [11-13]. An OCT system is essentially a Michelson

interferometer with a sample in one arm and a continuously variable delay line in the other arm. In the sample arm objective lens is used to collimate and focus the beam on the sample while a simple collimator is used in the reference arm. Especially in the case of RSODL, due to the different bulk optic elements used in both arms, usually undesirable artifacts appear in the OCT image unless the dispersion imbalance between the arms is cancelled. In order to compensate the dispersion imbalance, either extra optical components are deployed in the reference arm or the OCT image is post-processed to remove the artifacts. The proposed delay line consists of two CFBGs cascaded in the opposite direction with one of the CFBG being stretched to obtain a variable delay. The most interesting feature of this technique is the amplified optical delay. A small stretch applied on a fiber grating is amplified and gives a large optical delay because of the distributive reflection property of the CFBG.

Before going through detailed mathematical analysis of the proposed scheme, it might be helpful to have an intuitive understanding of the principle governing the scheme. Owing to the chirping, different wavelength components λ_1 and λ_2 of an incident beam will be reflected at different locations z_1 and z_2 in both CFBGs measured from the shorter period side as shown in Fig. 2. The λ_1 wavelength component, for instance, travels a distance z_1 in CFBG1 and a distance $L-z_1$ in CFBG2. Thus, the total traveling distance in both gratings becomes L , where both CFBGs are assumed to be identical and have the same length L . The same thing happens with the wavelength components λ_2 . Therefore, for any wavelength component the optical path length (OPL) suffered within both gratings becomes $2n_{\text{eff}}L$, where the factor 2 is added to include the round trip. Note that the delay occurred by traveling through the fiber between the gratings is not included. Interesting point to be noted is that all wavelength components suffer the same amount of OPLs within the gratings. However, when one of the CFBG is stretched or elongated, the reflection points in the gratings will be shifted increasing the delay. We will show that the amount of the shift depends on the chirping ratio and is much larger than the strain applied on the fiber. When a CFBG is stretched uniformly, its chirping ratio and the dispersive properties are not affected, which enables wavelength independent variable optical delay. Therefore wavelength independent optical delay property is preserved under strain but a gain in reflection position is obtained. The enhanced shift in the reflection points is the key concept of this scheme, whose detail discussion is followed.

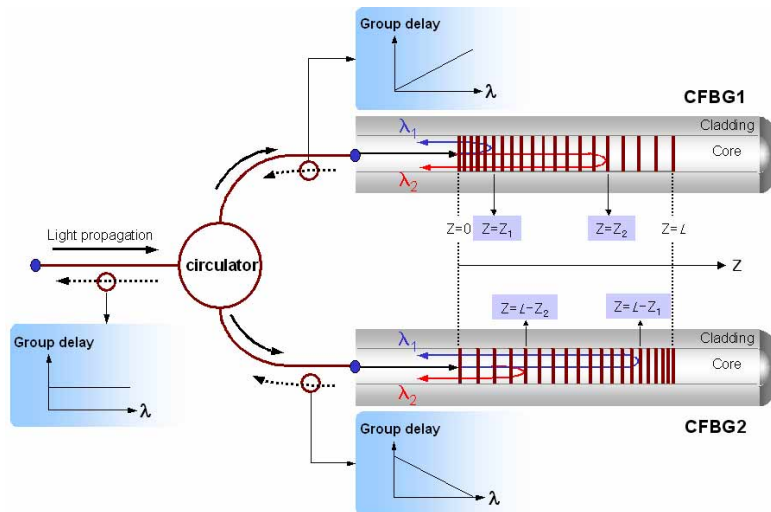


Fig. 2. The dispersion cancellation scheme in a pair of CFBGs cascaded reversely.

We can also understand the wavelength-independent nature of the delay line by considering the dispersion curves of the gratings. When a CFBG is linearly chirped, it has a linear group

delay as shown in the upper inset of Fig. 2. When a light is launched from the opposite direction of the identical CFBG, the slope of the dispersion curve remains the same but the sign changes as can be seen in the lower inset of the figure. Hence, when the light is launched into two identical CFBGs cascaded in the opposite direction, the dispersion associated with the CFBGs is canceled with each other and becomes flat, as depicted in Fig. 5. When a CFBG is stretched, the associated group delay curve is shifted to longer wavelengths without any change of slope as shown in Fig. 6(a). Thus stretching a grating will not disturb the dispersion cancellation. When a grating is being stretched, the flat group delay curve shown in Fig. 5 moves up corresponding to the amplified delay obtained by the AOFDL. It will be shown that the delay obtained is determined by the parameters of the gratings used. It should also be noted that for perfect dispersion cancellation, we require identical gratings that is very difficult in spite of the advancement of the grating fabrication technology due to the multitude of control parameters involved for the fabrication.

Adequate delay length to probe the sample and high speed scanning for real-time applications are determinant factors for the delay line to be applicable for OCT. Various techniques have been proposed and implemented [7,9,10,16,17] to obtain suitably large optical delay from a small physical displacement in ODL. Thus, we will show that the ODL we propose provides an adequate optical delay theoretically as well as experimentally to demonstrate its use for OCT applications.

The wavelength of the light beam reflected at a position z along a CFBG, which has the position dependent grating pitch of $\Lambda(z) = \Lambda_0 + \beta z$, is determined from Eq. (1) as

$$\lambda_B(z) = 2 n_{\text{eff}} (\Lambda_0 + \beta z), \quad (2)$$

where Λ_0 is a minimum (maximum) pitch for a positively (negatively) chirped CFBG. The positive (negative) chirping ratio β is in a unit of nm/mm. When we stretch the CFBG of a length L by an amount of an elongation length a , the grating pitch is elongated as

$$\Lambda'(z') = \alpha \Lambda_0 + \beta z'. \quad (3)$$

The elongation ratio α of the grating is defined by $(L+a)/L$ or $1 + \epsilon$. The strain ϵ applied on the fiber is defined as a/L . Note that despite applying strain, the chirping ratio β is not changed. The prime notation in Eq. (3) indicates that the parameters are related to strain. At the same time, the strain on fiber reduces the effective refractive index by a factor of $(1 - p_e \epsilon)$ due to elasto-optic coefficient p_e as given by [18]

$$n_{\text{eff}}' = n_{\text{eff}} (1 - p_e \epsilon). \quad (4)$$

Thus, by using the modified pitch and effective index, we obtain the modified expression for the Bragg wavelength of a strained CFBG as

$$\lambda_B'(z') = 2 n_{\text{eff}}' \Lambda'(z') = 2n(1 - p_e \epsilon) (\alpha \Lambda_0 + \beta z'). \quad (5)$$

Note that n_{eff} is replaced by n in the above equation for convenience and simplicity.

If a particular wavelength component λ of light is reflected at a position z in an unstretched grating, it will be reflected at a distance z' when the grating is stretched. Therefore, the OPL in the stretched CFBG becomes

$$OPL = n' z' = n(1 - p_e \epsilon) \frac{1}{\beta} \left\{ \left(\frac{\lambda_B'}{2n(1 - p_e \epsilon)} \right) - \alpha \Lambda_0 \right\}. \quad (6)$$

Since the Bragg wavelength λ_B' of Eq. (5) is the same as the one λ_B of Eq. (2) in this case, Eq. (6) becomes

$$OPL = n(1 - p_e \varepsilon) \frac{1}{\beta} \left\{ \left(\frac{\Lambda_0 + \beta z}{1 - p_e \varepsilon} \right) - (1 + \varepsilon) \Lambda_0 \right\}. \quad (7)$$

Expanding it becomes

$$OPL = n' z' = nz - \frac{n\Lambda_0}{\beta} (1 - p_e) \varepsilon + O(\varepsilon^2). \quad (8)$$

Therefore, the optical path length difference (OPD) obtained by stretching the CFBG is calculated by taking the difference between the OPL of the stretched one given by Eq. (8) and the un-stretched one nz . Neglecting the second order term of strain $O(\varepsilon^2)$, we have the round trip OPD as

$$2 \cdot OPD = 2(n' z' - nz) \approx -2 \frac{n\Lambda_0}{\beta} (1 - p_e) \varepsilon. \quad (9)$$

Usually the maximum strain applicable on an optical fiber is less than 1%, thus neglecting the second order term $O(\varepsilon^2)$ in Eq. (9) can be acceptable. The chirping ratio β can be expressed with the measurable grating parameters as

$$\beta = \frac{\Lambda_m - \Lambda_0}{L} = \frac{\lambda_m - \lambda_0}{2nL} = \frac{\Delta\lambda}{2nL}, \quad (10)$$

where Λ_m and λ_m are the maximum grating period and the maximum Bragg wavelength of the CFBG, respectively while $\Delta\lambda$ is the spectral bandwidth of the grating. By using Eq. (10) and the definition of applied strain ε , Eq. (9) is simplified as

$$2 \cdot OPD \approx -2n \frac{\lambda_0}{\Delta\lambda} (1 - p_e) a. \quad (11)$$

The equation states that stretching a CFBG by a length a provides a delay amplified by a factor of γ defined by

$$\gamma \equiv n(1 - p_e) \frac{\lambda_0}{\Delta\lambda}. \quad (12)$$

The factor γ , which is proportional to the ratio of the starting wavelength and the bandwidth of the CFBG, plays a role of gain in OPL. In other words, when the fiber is stretched by a length a , the induced optical delay is increased by a factor γ . If $\gamma \gg 1$, with a small stretching we can effectively get a large OPD. The minus sign in Eq. (11) means the phase of the operation. When both CFBGs are reversed or the strain is applied on the CFBG2 instead of CFBG1 in Fig. 2, the sign becomes positive.

Since the amplification factor γ strongly depends on the grating parameters, appropriate grating parameters must be chosen to obtain the required maximum delay. A large amplified delay can be obtained easily by making the bandwidth of the CFBG small, which can be easily appreciated with Eq. (12). However, such a choice will seriously degrade the resolution

of the OCT images that is inversely proportional to the bandwidth of the source. The CFBGs in the AFODL act like reflectors and thus using gratings with narrow bandwidth amounts to reduction of the source bandwidth. Therefore, we should consider appropriate trade-off between the amplification factor and the resolution in choosing the grating parameters for the delay line. Since the amplified optical delay possessing a constant amplification factor γ is linearly proportional to elongation length a , a variable delay line having good linearity and high repetition rate, can be achieved by using a PZT-based linear fiber stretcher to stretch the grating.

3. The implementation and characterization of the delay line

We used CFBG centered at 1330 nm to obtain the OCT images since the resolution of OCT is higher at lower wavelengths. However, we used gratings centered at 1550nm to demonstrate the dispersion properties of the delay line since the dispersion analyzer available (Advantest, Q7760) operates only in spectral band around 1550 nm. Each 4-cm long CFBG had a high reflectivity (>90%) and a 50-nm 3-dB spectral bandwidth. The measurement results are summarized in the following section.

The schematic of the OCT system with the proposed AOFDL is shown in Fig. 3. The 3 dB coupler shown in the figure aids in dividing and directing the source power in to the sample and reference arms and re-combine them after being reflected from the respective arms. The interference signal thus obtained by recombining the signals from the sample and reference arms is detected with a photo detector and processed to obtain the information about the sample. To measure the optical delay acquired from the AFODL by stretching the grating, we used the fiber delay line as a sample in the fiber based OCT system with conventional flat mirror mounted on a translational stage (PI) as the delay element in the reference arm. An amplified spontaneous emission (ASE) source (Thorlabs), which delivered 5-mW optical power with a bandwidth (FWHM) of 25-nm about 1560-nm center wavelength, was employed as source. Stretching of the CFBG is done by mounting the grating on a translational stage (Newport) with fiber-chucks. The translation stage on which mirror is mounted and set to oscillate at a repetition rate of 1 Hz over a 6 mm range to provide the variable delay. The interferograms were measured with and without stretching the grating and compared with each other and are presented in Fig. 6(b).

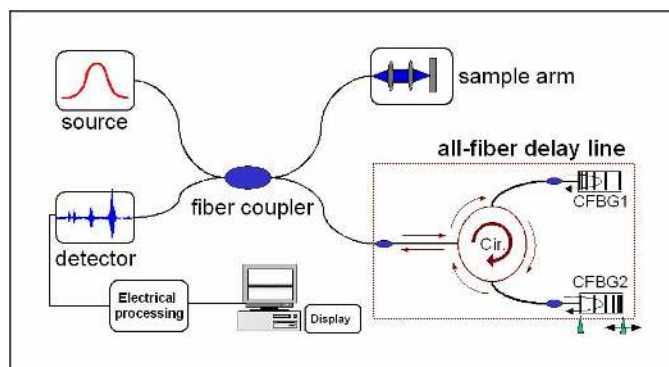


Fig. 3. The schematic of the proposed AFODL

Finally, images of the biological samples are obtained using the fiber grating based fiber delay line in the OCT system as shown in Fig. 3. As mentioned previously, we used another pair of gratings for the OCT imaging. For better OCT performance, we have used CFBGs with center wavelength at 1300 nm wavelength. The gratings are purchased from Bragg Photonics and are 4-cm long with 45 nm FWHM bandwidth and > 70 % reflectivity. Superluminescent diode (SLD) (1300-nm center wavelength, 50-nm spectral bandwidth at FWHM, 5-mW optical power, Kamelian Ltd.) is used as the broadband source.

A PZT-driven fiber stretcher was designed to hold the fiber straight and apply strain. The one-inch long PZT (Thorlabs) supports a maximum displacement of 20 μm , which was not long enough for OCT imaging. Thus, a custom-made flexure structure was employed to amplify the small displacement, and obtain a maximum displacement of about 100 μm . The PZT having a resonant frequency of 69-kHz was driven by both a high voltage controller (Thorlabs) and a function generator (Agilent). The fiber-stretching assembly is shown on the left side of Fig. 4. A sinusoidal signal (not triangular) was used to control the PZT motion, to avoid vibration of the fiber that can arise at the turning points of oscillation due to abrupt change of direction of motion. Further, the repetition rate was maintained at 6 Hz for the same reason. However, the limit in the scanning speed was not in the scheme of the proposed method but was in the designing of the fiber stretcher. A repetition rate faster than a few kHz is possible with the scheme.

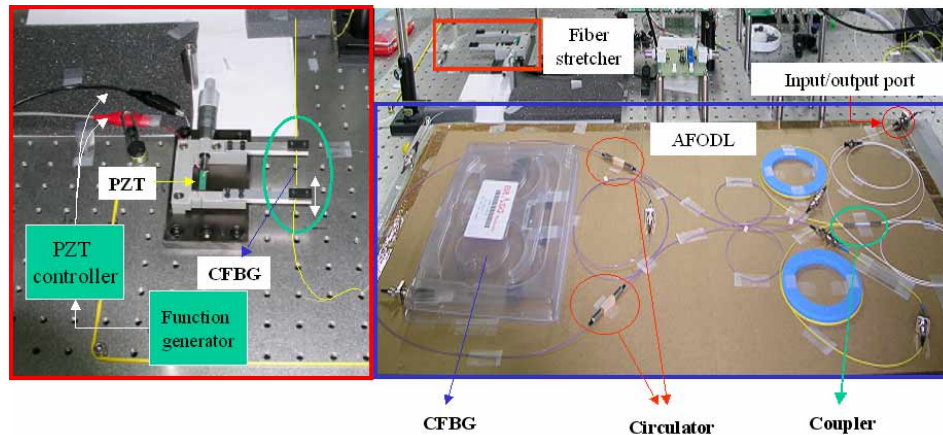


Fig. 4. A fiber stretching assembly driven by a PZT (red box) and an implemented AFODL (blue box) using fiber optic components such as fiber gratings, coupler, and circulators.

4. The experimental results

Figure 5 shows the dispersion curves of the individual CFBGs that form the delay line and the fiber delay line formed by cascading them.

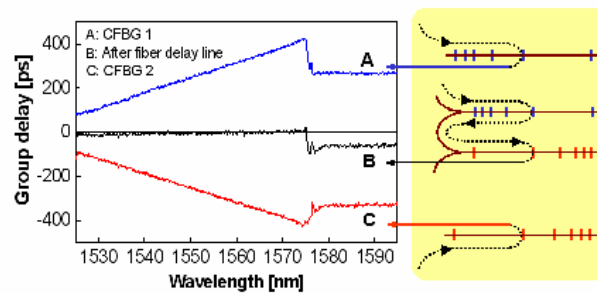


Fig. 5. The measured group delay for each CFBG and the cascaded CFBGs

The schematic of the corresponding gratings from which the dispersion curve is measured is shown on the right of Fig. 5. The dispersions of the CFBGs cancel each other in the delay line. However, careful observation shows that the dispersion is not completely

cancelled and is not zero. There still exists non-zero slope in the group delay curve B. This is believed to be because of non-identical gratings used in the delay line. Even though both CFBGs were designed to be identical, they were not exactly the same especially in terms of dispersion slope. The effect of stretching the CFBG is revealed in the dispersion curves measured before and after stretching a CFBG. As can be seen from Fig. 6(a), the dispersion slope is not changed by stretching and is merely shifted to longer wavelengths. The difference between the curve A and B was depicted with curve C that indicates that when a CFBG is stretched, it produces an appreciable amount of wavelength independent delay over the entire bandwidth of the CFBG.

Figure 6(b) shows two overlapped interferograms obtained with the OCT system in which conventional moving mirror is used as delay line and the CFBG based fiber delay line as sample. The two interferograms are obtained with and without strain on one of the CFBG. The stretch applied is 100 μm . The horizontal axis in an interferogram corresponds to the path length difference between the two arms obtained by the moving mirror. The shift of interferogram when the CFBG is stretched indicates the increase in the delay obtained by stretching the grating. The shift in the interferogram position by 2.5 mm with only 100 μm stretching of the grating affirms the amplified delay property of the fiber delay line. A delay of 2.5 mm for 100 μm strain on the CFBG corresponds to an amplification factor of 25.

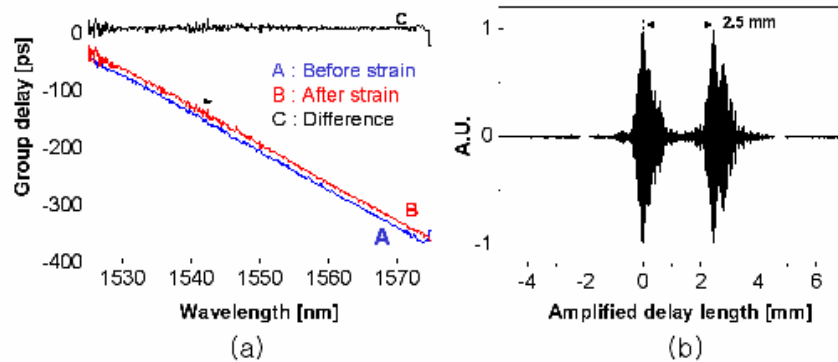


Fig. 6. (a) A shift of group delay induced by strain on a CFBG. The dispersion slope was not changed. (b) An amplified optical delay length of 2.5 mm obtained by stretching by 100 μm .

However, theoretically we expected an amplification factor of 35 from Eq. (12) for the parameters (1.45 for n , 0.23 for p_e , 1525-nm for λ_0 , and 50-nm for $\Delta\lambda$) of used CFBG. The discrepancy between the theoretical and the measured amplification factors is believed to be caused by slipping of fiber when it was under strain. Although the amplification factor is smaller than expected one, it is still in good agreement within the experimental errors.

As already mentioned we used another pair of CFBG pair centered around 1300 nm for OCT imaging. The induced OPD was measured for the delay line made from these pair of gratings, too. However, this time the grating to be stretched is mounted on the custom-designed flexure system and stretched using the PZT embedded in the flexure system. Variable strain is applied by controlling the voltage and the results are depicted in Fig. 7. With the maximum driving voltage of 150 V, the PZT provides a displacement of 20 μm . However, with the aid of flexure system, we could obtain a maximum displacement of 100 μm . From the figure, we can see that at the maximum driving voltage that corresponds to a stretch of 100 μm , an optical delay of 3.1 mm is obtained. Therefore, we can say that with the second CFBG pair we have achieved the amplification factor γ as 31. The theoretical amplification factor for this setup is calculated to be 32 (with 1.45 for n , 0.22 for p_e , starting wavelength of 1280 nm, and spectral bandwidth of 45 nm), which is well matched to the experimental one of 31.

Note that there was a difference of ~ 1.0 mm between the theoretical and experimental values of the OPD presented in Fig. 6, while it was only 0.1 mm for the data presented in Fig. 7. The reason is that in obtaining the data presented in Fig. 6, the fiber was stretched with a motor-driven translation stage while a custom-made fiber stretching assembly was used for the later one. The custom-made fiber-holder in the flexure could secure the fiber in position when it is being stretched without being slipped. However, Fig. 7 shows that the variation of optical delay is not linear with the voltage applied to the PZT. This deviation from linearity is due to the hysteresis of the PZT, which can be improved by operating the PZT in closed-loop. Although operation in the closed-loop mode may reduce scanning speed, a PZT operating at few kHz in feedback mode is still commercially available. Therefore PZT operation in feedback mode does not hamper the real-time performance in OCT imaging.

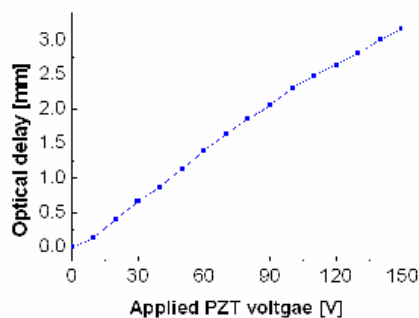


Fig. 7. Optical delay length measured with respect to the voltage applied on the PZT.

Up to now, the AFODL is used as a sample under test. From now on, we present several OCT images obtained with the AFODL as a scanning device in the reference arm of an OCT system. As samples, we have used a mirror, a cover glass, a tooth and a fish eye.

Figure 8(a) shows the interferogram obtained from a mirror, a single surface sample. The FWHM of the interferogram, which is a measure of axial resolution was measured to be ~ 100 μm . Compared with that of Fig. 6(b), the axial resolution was improved further. We attribute the enhanced performance to the use of the SLED source having shorter center wavelength and larger bandwidth than that of ASE source used for Fig. 6(b). By utilization of designed fiber stretcher to secure fiber holder and give smooth stretching, the broadening of the interferogram was also suppressed. The CFBG pair used for obtaining Fig. 8(a) were designed to have a little bit lower reflectivity than the ones for Fig. 6(b) with the hope of getting a more linear chirping and a lower group delay ripple (GDR). To avoid the difficulty in preparation of identical CFBG pair, we are also considering a fiber delay line based on a single CFBG not a pair.

The FWHM is related to the bandwidth and center wavelength of the source. The theoretical value for our source (50 nm bandwidth source operating at 1300 nm) is ~ 15 μm . The difference between the theoretical and the experimental values can be attributed to mainly three reasons. Firstly, there is a dispersion imbalance between the reference and the sample arms due to extra bulk optics. In the reference arm, we have not used any bulk optic element while the sample arm has a collimator and a focusing lens that may cause the dispersion imbalance. Secondly, dispersion of the CFBGs may not be identical which may add to the dispersion imbalance. This can be reduced by tuning the dispersion of the gratings without changing its central wavelength [19, 20]. Further, GDR cannot be completely cancelled. In general, the ripple frequency is not uniform against the wavelength [19, 20], thus just simply juxtaposing two identical CFBGs in the reverse direction is not good enough to be completely free from the effect of the GDR. However, the GDR can be reduced by adopting an

appropriate apodization in the index profile of the CFBG and by minimizing errors in the fabrication process [21, 22]. We can also think of an effect of non-linear chirping instead of that of linear. If a CFBG had a higher order chirping deviated from linear curve, the stretching the fiber would yield the wavelength dependent dispersion slope of the grating, which might induce the broadening. We are now investigating the effect of the higher order chirping on delay performance.

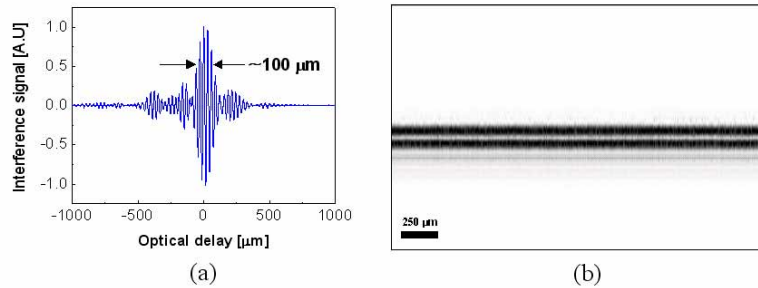


Fig. 8. (a) The interferogram of a single mirror surface. (b) The OCT image of a cover glass having a thickness of 100 μm . Both figures were taken by utilizing the proposed delay line.

A 2-D OCT image ($1,000 \times 10,000$ pixels) of a cover glass (150- μm thick, $n = 1.5$ at 1300 nm) acquired from the OCT system is shown in Fig. 8(b). The transverse and the axial resolutions of the system were 5 and 100 μm , respectively and the sensitivity or dynamic range was measured to be about 50dB. Even though the axial resolution was poor, it was good enough to distinguish the two surfaces of the cover glass. The nonlinear responsibility of the device originated from the hysteresis can give distortion in the OCT image. In the cover-glass image, due to this nonlinearity problem, the thickness of the glass was distorted with maintaining the smoothness. This problem can be simply overcome by doing software manipulation if we measure the exact hysteresis curve of the device. This measurement is believed to suggest the potential of the CFBG-assisted delay line in an OCT system.

To validate the performance of the system, biomedical samples have been used for OCT imaging. Figure 9 shows the photo image (a) of the cross-section of a molar tooth and its OCT image (b) taken with the setup shown in Fig. 3. The boundary between the enamel and the dentin regions of the tooth is well distinguished in the OCT image (b). The cross-sectional photo image of the sample was obtained by cutting the sample after obtaining the OCT image.

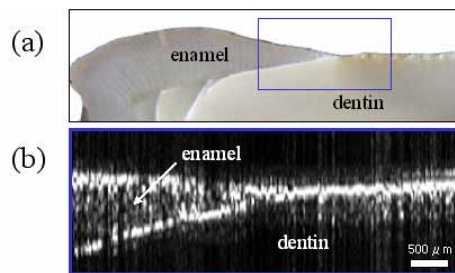


Fig. 9. (a) Cross-sectional photo image of a molar. (b) Its OCT image taken by utilizing the proposed AFODL. Pixel size and resolution are $500 \times 5,000$ and $10 \times 100 \mu\text{m}$, respectively.

Finally, with the proposed AFODL, the OCT image of a fish eye was taken. Fish was chosen due to the easy availability and the similarity to that of a human in the structure. Figure 10(a) shows the cornea of the fish. The upper and the lower layers of the cornea are distinguishable,

thus it can be used to evaluate the thickness and uniformity of the cornea layer. Figure 10(b) is the OCT image for the iris of the same sample. Since the limited scanning depth due to sinusoidal operation of PZT could not cover whole anterior chamber of the fish eye sample in the one-shot axial scanning. For this reason, we have imaged the cornea and iris separately. The abrupt change in the image is due to the boundary between the iris (lower left line) and skin of the fish (upper right line). Both Images have the same number of pixels ($1,000 \times 10,000$) and have been obtained with a resolution of $10 \mu\text{m} \times 100 \mu\text{m}$ in transverse and axial directions, respectively.

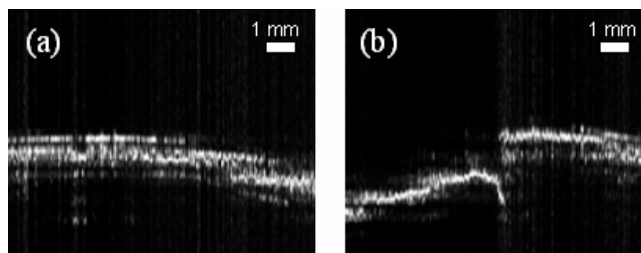


Fig. 10. (a) OCT image for the cornea of a fish eye and (b) the iris of the same sample.

5. Conclusions

We have implemented an all-fiber optical delay line (AFODL) based on chirped fiber Bragg gratings (CFBGs). The amplified delay property and non-dispersive features of the scheme under strain, which are based on the distributed reflection property of a CFBG, are discussed analytically and also verified experimentally. Although the group delay curve was not perfectly flat due to non-identical CFBGs used in the experiment, the flat delay curve is not severely degraded and the results are encouraging. During the stretching of a CFBG, net dispersion is varied without changing of slope of linear group delay and induces optical delay that is amplified being proportional to the ratio of the starting wavelength and reflection bandwidth. We obtained an optical delay of 3.1 mm by stretching a CFBG by $100 \mu\text{m}$, which amounts to an amplification factor of 31 while the theoretically predicted value is 32. The severe broadening in the interferogram is believed to be due to the residual dispersion owing to the incomplete dispersion compensation caused by non-identical CFBGs, which can be improved by using identical CFBGs.

The implemented AFODL has been used for imaging transparent glass plate (cover glass) and biomedical samples (molar tooth and fish eye). The obtained OCT images confirmed the feasibility of the AFODL in an OCT system. The proposed technique has the potential of realizing a cost-effective and high speed AFODL by using a high-repetition rate PZT and an efficient flexure for the fiber stretching.

Acknowledgments

This work was supported in part by the Korea Science and Engineering Foundation (KOSEF) through grant No. R01-2001-000-00327-0 from the Basic Program the Ultrafast Fiber-Optic Networks (UFON) Research Center at Gwangju Institute of Science and Technology (GIST), by the Korean Ministry of Education (MOE) through the BK-21 Project, and by the Ministry of Science and Technology (MOST) through the Strategic National R&D program (grant No. M1033000001-03B3700-00110), and through the Korea-China Joint Research Project (grant No. M60403000076-04A0100-01310), Korea. We also acknowledge Korea Photonics Technology Institute (KOPTI) for providing the dispersion measurement facility.